Project 078 Contrail Avoidance Decision Support and Evaluation

Massachusetts Institute of Technology

Project Lead Investigator

P.I.: Steven R. H. Barrett
Professor of Aeronautics and Astronautics
Director, Laboratory for Aviation and the Environment
Massachusetts Institute of Technology
77 Massachusetts Ave, Building 33-207, Cambridge, MA 02139
617-253-2727
sbarrett@mit.edu

University Participants

Massachusetts Institute of Technology

- P.I.: Prof. Steven R. H. Barrett
- FAA Award Number: 13-C-AJFE-MIT, Amendment Nos. 086 and 100
- Period of Performance: October 1, 2021 to September 19, 2023
- Reporting Period: October 1, 2021 to September 30, 2022
- Tasks:
    1. Contrail Forecast Module
    2. Contrail Identification Module
    3. Contrail Radiation Module
    4. Trajectory Planning Module

Project Funding Level

This project received $1,100,000 in FAA funding and $1,100,000 in matching funds. Sources of matching are approximately $168,000 from Massachusetts Institute of Technology (MIT), plus third-party in-kind contributions of $469,000 from Savion Aerospace Corp. and $463,000 from Google, LLC.

Investigation Team

Principal Investigator:	Prof. Steven Barrett (MIT) (all tasks)
Co-Investigators:	Dr. Sebastian Eastham (MIT) (all tasks)
	Dr. Florian Allroggen (MIT) (all tasks)
	Dr. Raymond Speth (MIT) (all tasks)
	Dr. Jayant Sabnis (MIT) (all tasks)
Graduate Research Assistants:	Jad Elmourad (MIT) (Tasks 3-4)
	Vincent Meijer (MIT) (Tasks 1-2)
	Louis Robion (MIT) (Tasks 1-2)

Project Overview

Contrails are white, line-shaped ice clouds that form behind aircraft. Contrails and subsequent contrail cirrus are thought to account for approximately one half of the climate warming attributable to aviation. Contrail avoidance through vertical and horizontal flight path changes is estimated to cause fuel burn penalties of a few percent. Thus, contrail avoidance is a potentially cost-effective way to mitigate the climate impacts of aviation. However, contrail avoidance has not been demonstrated at scale, and a comprehensive toolset to support this approach has not been developed. The goal of this project is to create a contrail avoidance decision support and evaluation tool that can be utilized to optimize and evaluate

the benefits, costs, and practicality of contrail avoidance. In addition, subject to agreement with industry partners, we will seek to test contrail avoidance in a way that has no implications for air traffic control or safety.

This project aims to satisfy four specific objectives: (a) develop the capabilities necessary to predict the formation and impacts of contrails from a given flight, (b) evaluate the financial costs and environmental benefits of deviating from a given path to avoid a contrail, including uncertainty, (c) integrate these capabilities into an operational tool that can provide near-real-time estimates of the costs and benefits of a contrail avoidance action, informed by automated, coordinated observational analysis and modeling, and (d) evaluate the effectiveness of these tools in a safe, scientifically sound real-world experiment.

The objectives outlined above will be met through a work program that comprises the following tasks:

1. Contrail Forecast Module
2. Contrail Identification Module
3. Contrail Radiation Module
4. Trajectory Planning Module

The following tasks will be included under future periods of performance (not funded through the current submission) and will provide an outlook for follow-on work in future project years.

5. Cost–Benefit Evaluation Module
6. Airline Integration
7. Experiment Evaluation Module

The remainder of this document presents a description of the first four tasks, including research progress and next steps.

Task 1 - Contrail Forecast Module

Massachusetts Institute of Technology

Objective

The goal of Task 1 is to develop a contrail forecast module that predicts the likelihood of persistent contrail-forming conditions one day ahead, in the hours before the flight, and in real time during a flight. This module is intended to allow airlines to decide ahead of time whether flights may wish to use contrail avoidance, to file flight plans accounting for the best estimated cruise altitude, and to adjust in real time (subject to pilot workload and air traffic control constraints).

Research Approach

Prediction will be performed using a combination of U.S. agency meteorological forecasts and observational data, including prior satellite observations of contrails from earlier flights. We will begin by using meteorological data from the NASA Global Modeling and Assimilation Office Goddard Earth Observing System (GEOS) Forecast Product, which has a moderate resolution (0.25° latitude by 0.3125° longitude globally) and provides new 5- and 10-day forecasts each day (Rienecker et al., 2008). As the project progresses, we will evaluate regional products such as the National Oceanic and Atmospheric Administration High-Resolution Rapid Refresh (HRRR) system to provide greater resolution over the United States.

Evaluating existing forecasts

We evaluated the capability of existing numerical weather prediction (NWP) models to forecast persistent contrail formation areas (PCFAs). This evaluation was achieved by transforming the meteorological variables provided by these NWP models into a Boolean grid marking PCFAs. PCFA calculation relied on the Schmidt–Appleman criterion for contrail formation and the ice supersaturation criterion for contrail persistence. Together, we term these conditions "persistent contrail conditions" (PCCs). Additionally, we used a satellite-based contrail detection algorithm to evaluate the ground-truth PCFAs. By randomly sampling points on the grid and comparing these two sets of PCFAs, we evaluated the capability of NWP models to forecast PCFAs.

We used two metrics – precision and recall – which vary between 0 and 1, with 1 indicating optimal performance for a metric. Precision indicates the ratio of true positives to the sum of true positives and false positives. In other words, precision

indicates the number of times that the NWP model correctly forecasts a PCFA divided by the total number of times that the NWP model forecasts a PCFA. Recall indicates the ratio of true positives to the sum of true positives and false negatives. In other words, recall indicates the number of ground-truth PCFAs that the NWP model was able to forecast divided by the total number of ground-truth PCFAs (i.e., including those that the NWP model did not forecast).

We applied this procedure to the NWP product HRRR provided by the National Oceanic and Atmospheric Administration. The HRRR has 3-km resolution and is updated hourly. We found that the performance was low, with a precision mean below 1% and a recall mean below 50% (see Figure 1.1).

Furthermore, an evaluation of ECMWF Reanalysis v5 (ERA5) wind data was conducted because wind velocities and uncertainty play an important role for both contrail nowcasting and contrail-to-flight attribution (as discussed below). The wind uncertainty was quantified by comparing ERA5 values with Aircraft Meteorological Data Relay (AMDAR)-reported values. The results showed that ERA5 and AMDAR horizontal winds agreed within a root mean square error (RMSE) of less than 3 m/s (see Figure 1.2), which is expected given that these measurements are assimilated. We switched from modeling the wind uncertainty as a Gaussian distribution with constant standard deviation to using a standard deviation that is a linear function of the wind speed as shown below.

$$\sigma_{ERA5} = \alpha|u_{ERA5}| + \beta$$

where σ_{ERA5} is the standard deviation of the wind, u_{ERA5} is the wind velocity, and α and β are parameters determined by model fits to the data. We modeled the eastward and northward components of the wind independently. The resulting values for α and β are shown in Table 1.1.

Table 1.1. Values for the wind uncertainty model parameters.

Wind component	α [-]	β [m/s]
Eastward	0.0106	1.7
Northward	0.0878	1.15

We also assessed the performance of multiple techniques for wind data interpolation by artificially “coarsening” the ERA5 grid and comparing the interpolated wind values with those at the grid points that were removed. We found that bicubic interpolation in the horizontal, quadratic interpolation in the vertical, and linear interpolation in the temporal dimension performed best. The results of this evaluation will form part of the basis for incorporating uncertainty into PCFA forecasts, a key component of final tool development.

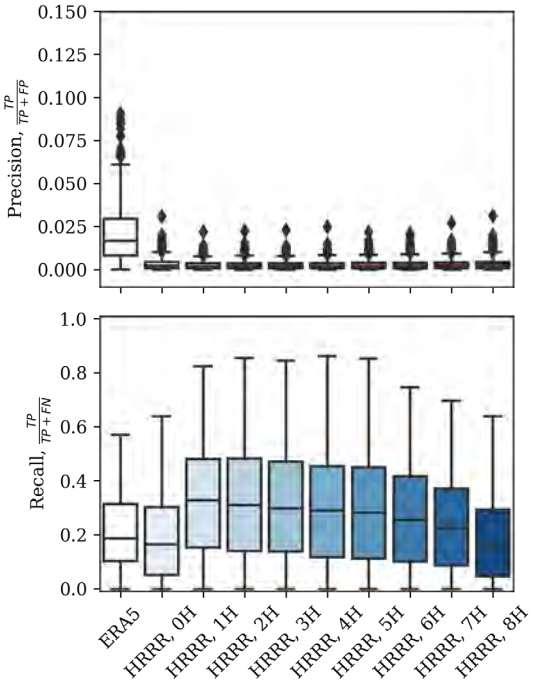

Figure 1.1. Preliminary estimate of the performance of the ECMWF Reanalysis v5 (ERA5) reanalysis and High-Resolution Rapid Refresh (HRRR) forecast, measured by recall (top) and precision (bottom), as a function of forecast lead time. The data represent 1,000 randomly sampled time points in 2018 and 2019. FN: false negative; FP: false positive; TP: true positive.

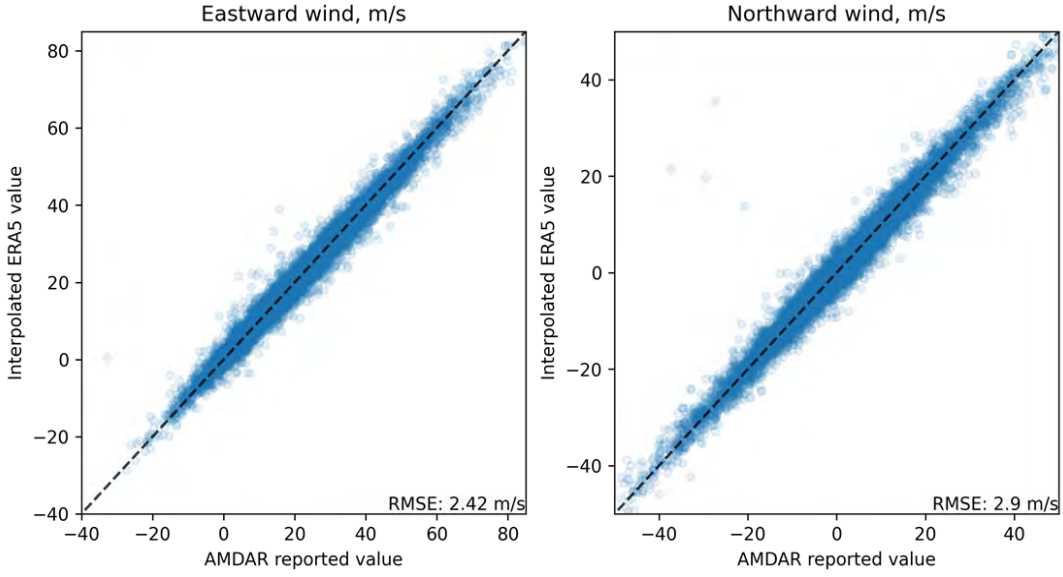

Figure 1.2. Comparison between ERA5 and Aircraft Meteorological Data Relay (AMDAR) horizontal winds. RMSE: root mean square error.

Development of contrail nowcasting

Because our metrics indicated that NWP data alone are not sufficient to accurately forecast PCFAs, we investigated nowcasting, which is an approach that uses recent contrail observations to forecast PCFAs. For example, if contrails were detected in region X, the nowcasting approach would forecast a PCFA in region X, at least for short lead times. The nowcasting approach can also include wind data to forecast the advection of the PCFA (see Figure 1.3). Because of this feature, the above-mentioned quantification of the ERA5 wind uncertainty was useful. The nowcasting approach relies heavily on the contrail identification module (see Task 2).

We investigated two approaches to nowcasting: Eulerian persistence and Lagrangian persistence (see Figure 1.3). In the Eulerian persistence approach, we assume that the region in which contrails are detected will continue to be a PCFA for the near-term future. In the Lagrangian persistence approach, the PCFAs move horizontally with the wind.

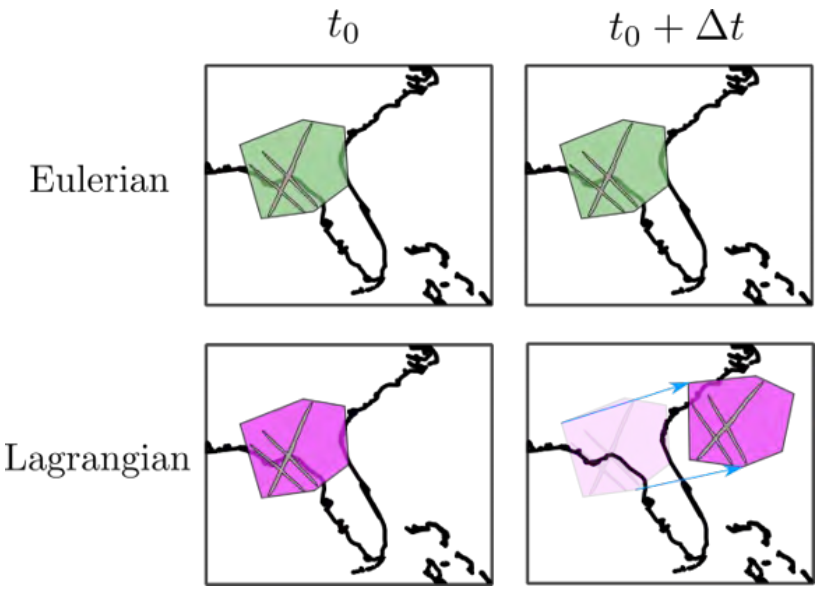

Figure 1.3. Schematic of two approaches to nowcasting: Eulerian and Lagrangian. The gray lines represent contrail detections whereas the regions in solid green and magenta indicate the location of persistent contrail formation areas that would be estimated by the nowcasting approach.

The performance of these two nowcasting approaches was compared with that of the two NWP-based models: ERA5 and HRRR. The result for the recall metric is shown in Figure 1.4. Compared with Figure 1.1, which shows a preliminary estimation of the HRR performance, Figure 1.4 only quantifies the recall metric because an accurate estimation of the precision metric depends on work being developed under Task 2, namely combining contrail observations with flight track data. As shown in Figure 1.4, and by definition, the nowcasting approaches initially have 100% recall. The plot shows that even though the performance of the nowcasting approaches deteriorates quickly with increased lead time, the nowcasting approaches are still better for lead times up to 2 h. The ERA5 performance is independent of the lead time (single reanalysis) whereas the HRRR performance improves with lead time (differences in assimilated data).

The superior performance of the Eulerian approach compared with the Lagrangian approach reflects three factors. Firstly, we know from visual analysis of contrail observations that PCFAs do not move at the same speed as the contrails themselves. Because contrails are advected by the wind, the PFCAs move at a separate speed, likely related to the factors that give rise to PCFAs in the first place. Secondly, we know that the wind data are imperfect, meaning that advection of the PCFAs based on wind data will also suffer from accumulating error. Finally, the definition of a PCFA based on observations is itself uncertain (see Task 2), which may introduce different biases for the two approaches.

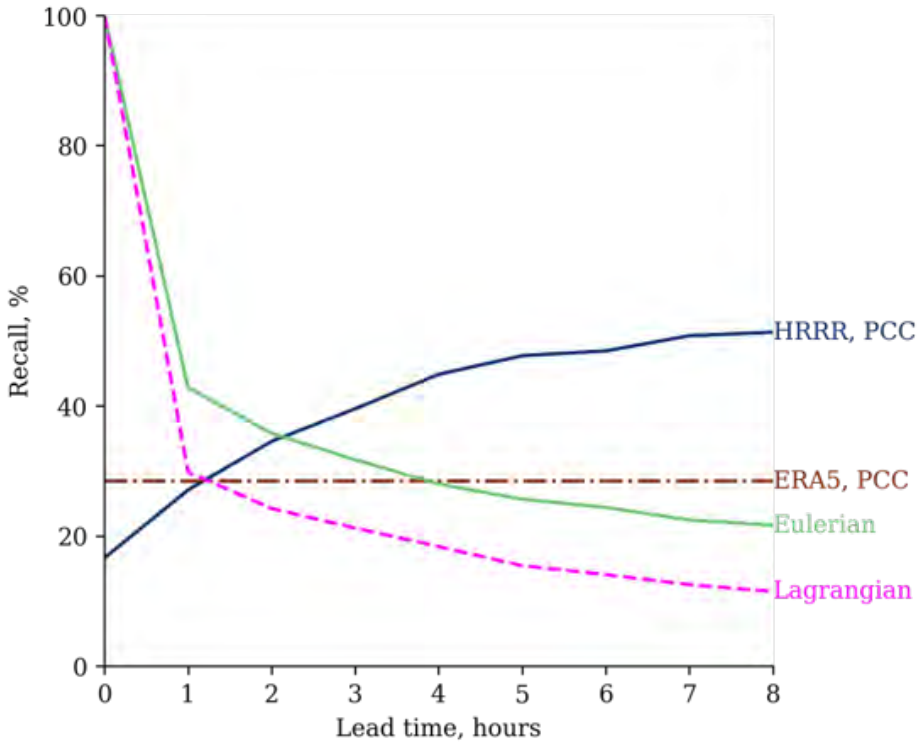

Figure 1.4. Evaluating the performance of various forecasting approaches as a function of lead time. HRRR: High-Resolution Rapid Refresh; PCC: persistent contrail condition; ERA5: ECMWF Reanalysis v5.

Based on this assessment, future tool development is focused on contrail nowcasting, with the goal of further leveraging observations rather than relying on NWP models.

Milestone

Milestone 1: Concept demonstration and first implementation of a contrail forecasting functionality for the FAA [*complete*].

Major Accomplishments

- Evaluated existing NWP models on their ability to predict contrail-forming regions
- Quantified errors in ERA5 wind velocity and wind shear data that could compromise flight attribution and nowcasting components
- Evaluated the performance of simple nowcasting approaches, comparing them with other NWP models

Publications

None.

Outreach Efforts

An oral presentation was given by Vincent Meijer at the 5th International Conference on Transport, Atmosphere and Climate in Munich, Germany, hosted by the German Aerospace Center.

Authors: Vincent R. Meijer, Sebastian D. Eastham, Steven R. H. Barrett
Title: Using satellite-based observations of contrails to inform contrail avoidance strategies
One-sentence summary: Comparison of satellite-based observations of contrails with numerical weather prediction data indicates that forecasts of persistent contrails are lacking. Short-term approaches that utilize observational data of contrails are shown to outperform numerical weather prediction models.
Date: June 29, 2022
Publication status: N/A

Awards
None.

Student Involvement
The research for this task was primarily conducted by Vincent Meijer with assistance from Louis Robion, both graduate research assistants at MIT. The communication of this research to the FAA was primarily conducted by Jad Elmourad, a graduate research assistant at MIT.

Plans for Next Period
- Develop and evaluate a nowcast of contrail-forming regions based on current inferred conditions, projected winds, and a physics-based understanding of contrail-forming regions.
- Use the improved contrail height estimates (see Task 2) to extend the nowcast of contrail observations from 2D to 3D.
- Evaluate the accuracy of forecasts in predicting contrail formation using the new approach developed under the contrail identification module.

References
Rienecker, M. M., Suarez, M. J., Todling, R., Bacmeister, J., Takacs, L., Liu, H. C., & Nielsen, J. E. (2008). The GEOS‐5 Data Assimilation System: Documentation of versions 5.0. 1 and 5.1. 0, and 5.2. 0 (NASA Tech. Rep. Series on Global Modeling and Data Assimilation, NASA/TM‐2008-104606, Vol. 27, 92 p.). *Greenbelt, MD: NASA Goddard Space Flight Center*.

Task 2 - Contrail Identification Module
Massachusetts Institute of Technology

Objective
The objective of Task 2 is to develop a real-time contrail identification module that locates contrails both horizontally and vertically. This module will be necessary to evaluate whether contrail avoidance has been successful. Furthermore, this module will enable contrail forecasting approaches that are based on contrail detections and that might prove to be more reliable for shorter lead times than approaches based on numerical weather forecasts. The initial version will use Geostationary Operational Environmental Satellite (GOES) observations combined with a deep learning approach developed by MIT (under NASA sponsorship) to identify contrails from space. Future developments could include other satellite products, ground observations, and other observations.

Research Approach
We started with a contrail detection algorithm based on satellite imagery from GOES-16. This algorithm was then used to develop a probabilistic estimate of the contrail-forming regions using a kernel density estimation (KDE) approach, building on prior NASA-funded work. Flight data were then integrated into the model to improve our estimates. These steps allowed the contrails to be located horizontally. Next, we initiated the development of a contrail height estimation algorithm. A validation dataset of contrail locations was created to improve the performance of the algorithms. Furthermore, we have started integrating temporal data into the contrail detection algorithm. This integration improves the temporal consistency of the contrail detections (i.e., a given contrail is detected in every frame of a series of images) and may allow contrails to be detected earlier. This latter piece of information would significantly improve our ability to determine which flight created the detected contrail and to therefore verify the success of contrail avoidance actions.

Probabilistic approach using KDE
The initial implementation of a contrail identification module, developed under prior NASA funding, relied on binary PCFAs. This implementation was achieved by mapping satellite-observed contrails onto a grid, estimating the region bounded by the observed contrails on the grid, and then transforming the grid into a set of polygons based on the density of contrail observations. However, we discovered two issues with this approach. First, contrail detections were not temporally consistent, which led to polygons that frequently changed shape. Second, this approach did not account for uncertainty in the detections and did not make use of prior knowledge about the shape of PCFA regions. For these reasons, we moved toward a probabilistic approach.

Instead of a binary map of PCFAs, we now use a contrail detection mask to generate a KDE. The idea behind this KDE is that each contrail "induces" its own probability distribution (the kernel) and that the distributions of multiple contrails may interact. One such example is the case of two contrails (see Figure 2.1), where the PCFA probability between the two contrails increases as they approach each other. The kernel is parametrized as a multivariate Gaussian distribution. These parameters can be used to encode prior knowledge on PCFAs. For example, using three different parameters, the shape of the induced KDE can be stretched along the contrail length, perpendicular to the contrail length, or in proportion to the contrail length.

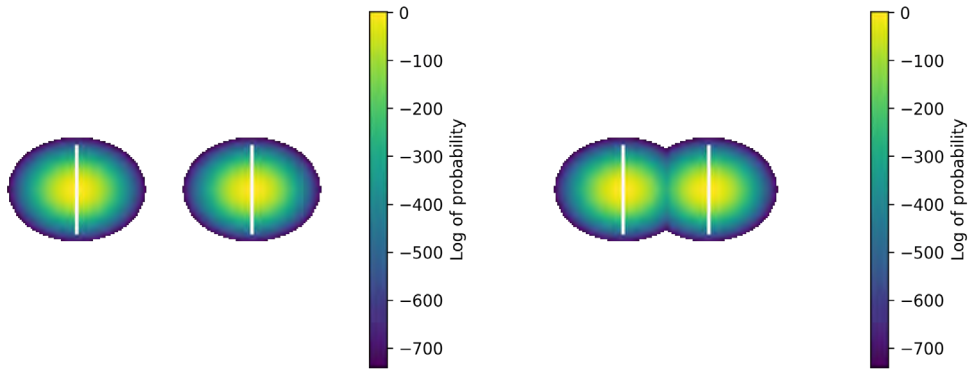

Figure 2.1. Example of kernel density estimates from contrail detections. The white lines represent contrail detections, and the colormap represents the probability of the detection being a persistent contrail formation area. The left plot shows two contrails that are far from each other. The right plot shows the interaction of two contrails close to each other.

Integration of flight data

Contrail detections provide information about contrail locations; however, for a location without any contrail detections, there are multiple possible scenarios. One possibility is that the region is not a contrail-forming region whereas the other possibility is that no flights have passed through that region. Without integrating flight data into our model, we are not able to differentiate between these two scenarios. Therefore, we investigated the integration of flight data to improve the probabilistic estimate of PCFA locations.

The advection of flight data was implemented in order to match flight locations at the time that a contrail is detected from the satellite. The advection of flight data uses ERA5 wind data, leveraging the ERA5 wind uncertainty model developed under Task 1 (discussed above).

The flight density data and probabilistic contrail detections can be combined by using Bayes' rule to improve our estimate of contrail regions. An example is shown in Figure 2.2. This approach provides the desired behavior in three ways. First, regions with contrail detections have a high probability of being a PCFA. Second, regions with no contrail detections but with high flight density have a low probability of being a PCFA. Finally, regions with no contrail detections and low flight density have an intermediate probability of being a PCFA. In the last case, the probability should revert to the climatological mean for PCFAs. This approach has shown promise but is still under development.

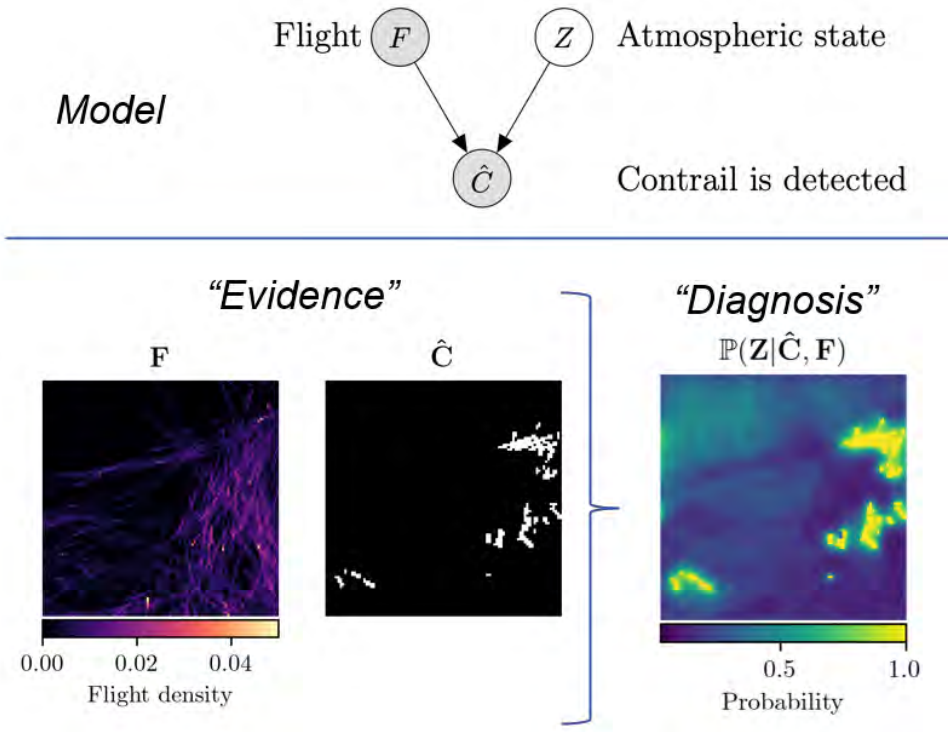

Figure 2.2. Example of applying Bayes' rule to derive the persistent contrail formation area (PCFA) probability by combining contrail detections with flight data. The three plots are maps of the same region, located within the contiguous United States (CONUS). The left plot represents flight density, the middle plot represents the contrail detections (with a threshold), and the right plot represents the estimated probability of a location being a PCFA.

Creation of a collocated contrail dataset

Under a prior grant, we developed an automated collocation procedure consisting of contrails detected and matched on both GOES Advanced Baseline Imager and NASA Cloud-Aerosol Lidar with Orthogonal Polarization (CALIOP) instruments. This procedure was applied to all 2018, 2019, 2020, and 2021 CALIOP overpasses, resulting in a validation dataset of approximately 3,200 contrail cross-sections. This dataset is the foundation of our validation efforts, as it provides a ground-truth dataset of contrail observations including longitude, latitude, altitude, time, width, and depth.

Development of a height estimation algorithm

Using the validation dataset described above, we performed a quantitative evaluation of state-of-the-art height estimation approaches. One such approach has been developed for cirrus clouds (Kox et al., 2012; Strandgren et al., 2017), but we found that it does not perform as well on contrails. We found that the RMSE in estimated contrail altitude was 3.3 km, approximately four-fold larger on the contrail-only dataset than the cirrus data test set. This precludes accurate identification of PCFA altitude, as PCFAs are thought to be on the order of only 500-1,000 m in vertical extent. As a result, we initiated the development of a height estimation algorithm targeted at contrails.

We explored two different machine-learning-based models: random forests and neural networks. We found that by training an algorithm directly on the contrail dataset, we were able to reduce the RMSE by a factor of 4–5 compared with the algorithm trained on the cirrus dataset, yielding the current RMSE of approximately 600 m. Work is ongoing to further reduce this error and to broaden our validation dataset. We are also expanding the contrail height estimation algorithm so that it outputs additional metrics related to the estimation uncertainty. An example from the algorithm's test set is shown in Figure 2.3.

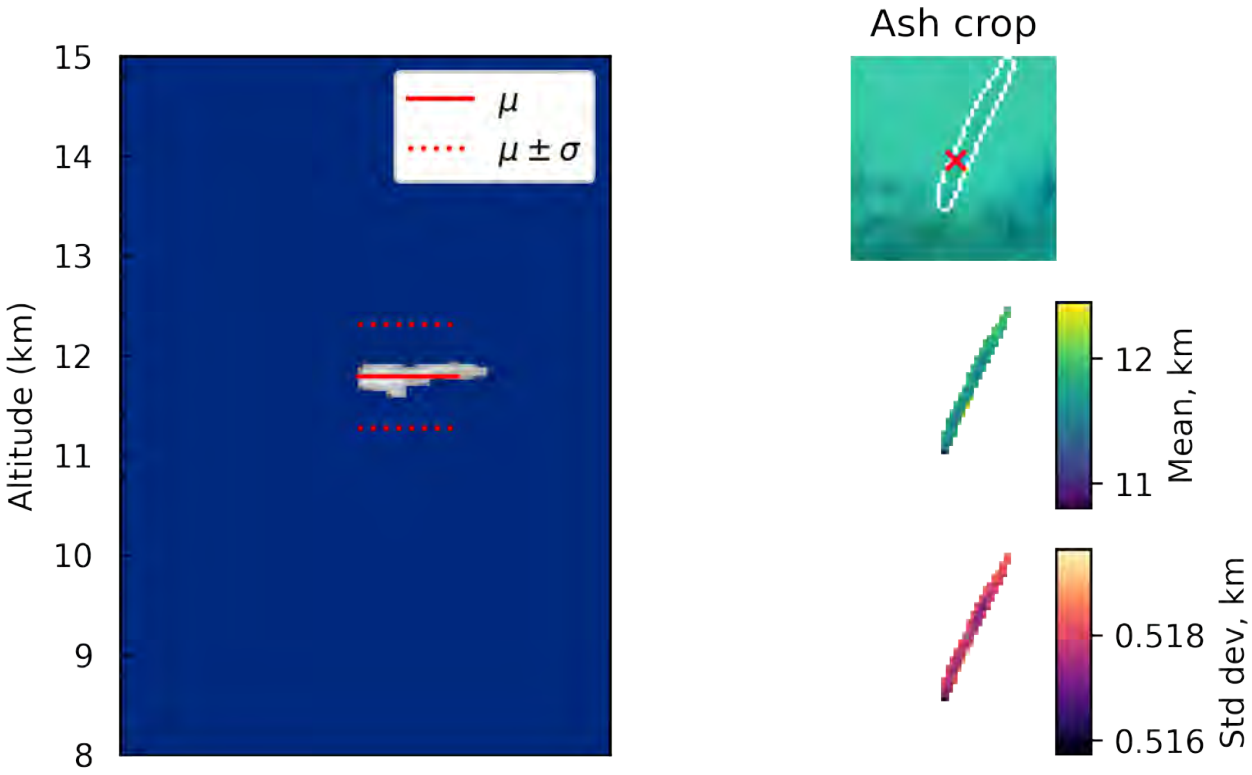

Figure 2.3. Example of contrail height estimation. The plot on the left shows a contrail cross-section observed by the Cloud–Aerosol Lidar with Orthogonal Polarization (CALIOP) instrument. The solid red line represents the mean height of the contrail estimated by the height estimation algorithm. The dashed red lines represent the mean ± one standard deviation. The top right image shows the boundary of the contrail detected on the Geostationary Operational Environmental Satellite (GOES) Advanced Baseline Imager. The "x" represents the GOES pixel that was collocated with the CALIOP data. The lower right figure shows the pixel-wise output of the height estimation algorithm; specifically, the mean height and standard deviation of the contrail are shown.

Integration of temporal data in contrail detections

Contrail detection masks produced by the detection algorithm are computed independently, meaning that a mask at time t+Δt does not use information provided by the detection mask at time t. For a sequence of consecutive GOES-16 images, this approach sometimes leads to temporal inconsistencies, where a contrail can be detected at t, not detected at t+5 min, and detected again at t+10 min. This motivated work under our NASA Atmospheric Composition Modeling and Analysis Program (ACMAP) grant to improve detections, which we are now leveraging, improving, and operationalizing in this work.

To increase the robustness of our contrail detections, in our NASA-funded ACMAP work, we began to implement a Kalman filtering approach to smooth the detection signal. This approach relies on our knowledge of advection, which governs the movement of contrails, and our observations, which correspond to the detection masks produced by the detection algorithm. By combining this information, we seek to construct a contrail detection signal that is more consistent in time than the detections alone.

We selected this approach because it is physics-based and does not require additional training data, as required by a machine learning model. A machine learning model would need to be trained with a large number of sequences of consecutive GOES images in which contrails are manually labeled. Creating a sufficiently large dataset to train such an algorithm would be difficult and very time-consuming. Having temporally robust consistent contrail detections may also enable us to identify new contrails on GOES images, which would facilitate the validation of a contrail avoidance strategy by simplifying the attribution of new contrails to the flights that produced them.

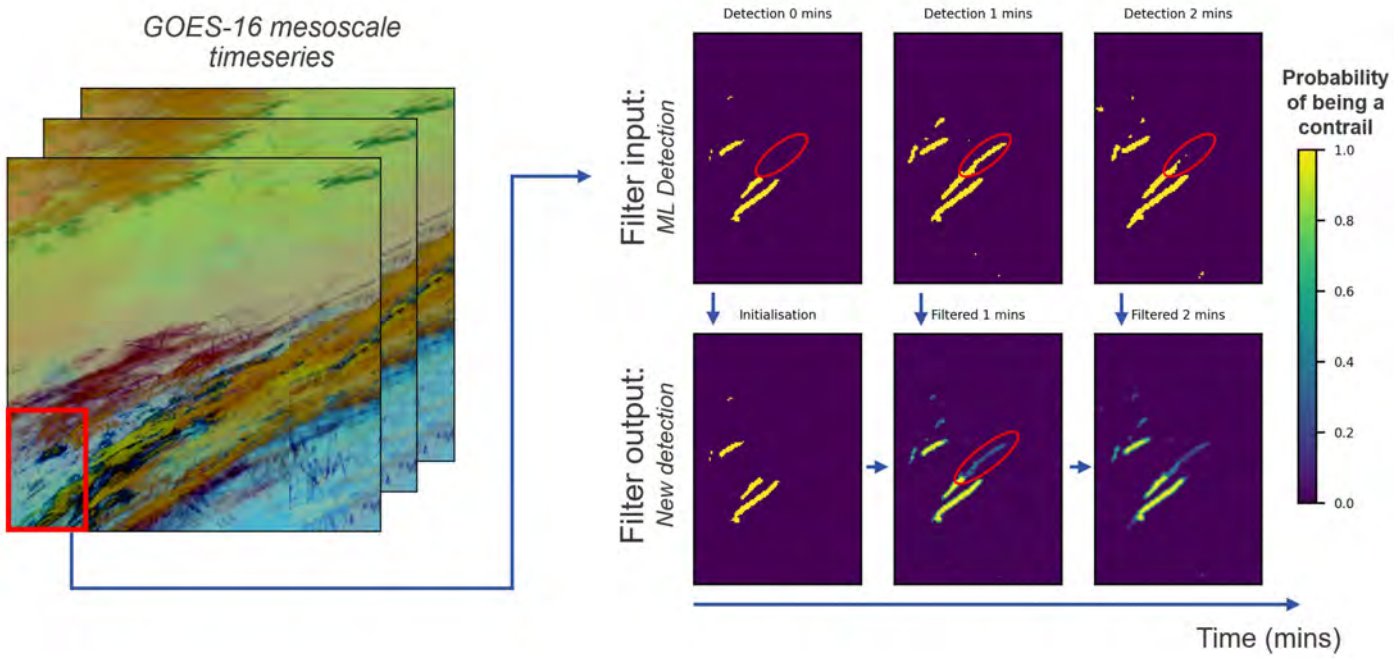

Figure 2.4. Example output of the prototype Kalman filter. Given a time series of Geostationary Operational Environmental Satellite 16 (GOES-16) mesoscale images, we can detect contrails using the machine learning detection algorithm. These contrail detection masks are then used as "observations" to compute filtered detections. Left plot: Sequence of ash transforms of GOES-16 images. Right plot: Diagram of the Kalman filter pipeline with contrail detection masks. Machine learning detections (top row) are used as an input to the filter. At each timestep, the filter computes a prediction of the next state based on the previous filtered output and combines it with the current machine learning detection. This produces a new "filtered detection." The red ovals on the top row highlight a clear false positive detection at T = 1 min. The red oval on the bottom row shows that the filtered product assigns a low probability of those pixels being contrails, effectively smoothing the detection signal. ML: machine learning.

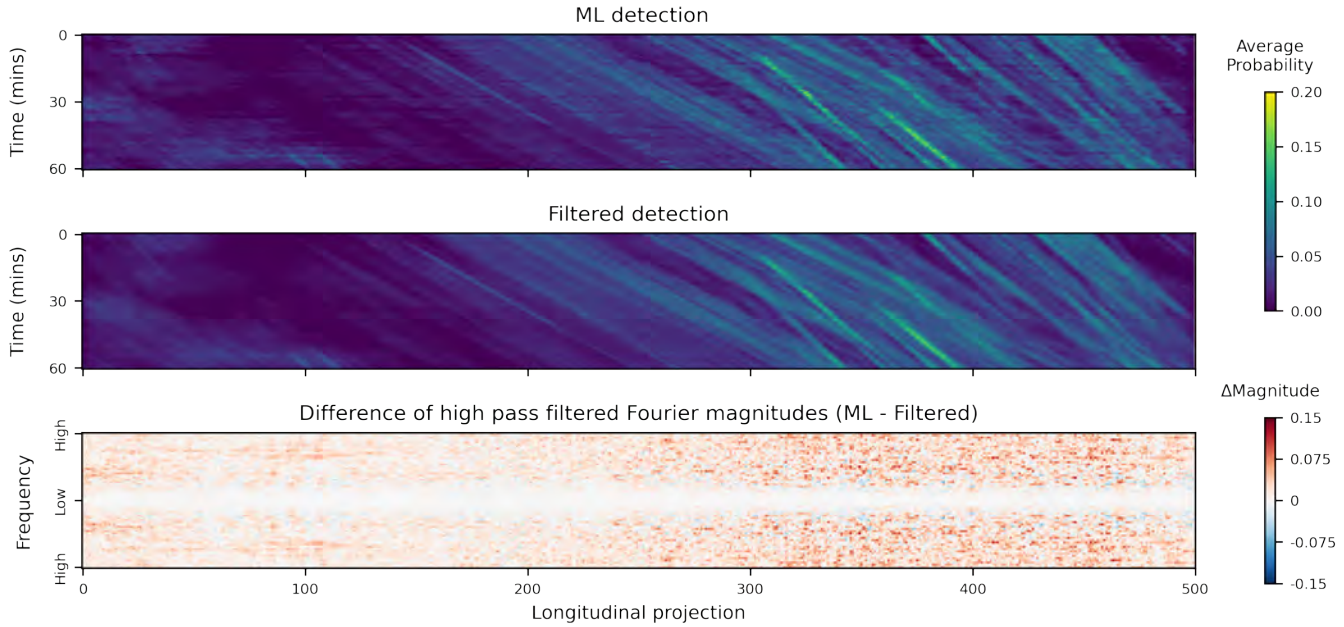

Figure 2.5. Two Hovmöller diagrams of a 60-min series of contrail detections and their Fourier transforms. The detection mask at each timestep is averaged along the vertical axis, and these data are then concatenated to present a time series of the average probability in that direction. We then compute the Fourier transform of each time series for both the machine learning detection and the filtered detections. By taking their difference in magnitude, we find that the machine learning detection time series contain substantially more high-frequency components than their filtered counterpart, showing the smoothing provided by the Kalman filter. ML: machine learning.

The final product of our ACMAP work was a prototype Kalman filter that was capable of smoothing detections, but that had not yet been validated against observations, tuned to improve performance, or leveraged to provide operational benefits. The work under ASCENT 78 aims to address these issues.

Creation of a contrail-labeled GOES mesoscale sequence

To evaluate the performance of the Kalman filtering approach, we started labeling a 2-h-long sequence of GOES mesoscale images. This GOES product provides images every minute and will allow us to compare a ground-truth sequence of contrail labels with those produced by the detection algorithm and Kalman filter.

This labeled sequence will first be used to tune and quantify the performance of the filter. For this step, we are currently exploring methods relying on Lagrangian advection of air parcels and wind data from numerical prediction models. Along the trajectory of an air parcel, the manual labels and filtered detections indicate whether a point is part of a contrail. We then compare the detection series of the filtered output and of the labels for that air parcel. We can tune and quantify the performance of the filter based on the similarity of the two series.

For operational use, if the filtered detection were consistent in time, the tracking of individual contrails would be easier. Tracking contrails over time would allow us to identify when a contrail has formed, which would facilitate matching the contrails to the aircraft that produced them, as it narrows the time window for potential “source” flights. To validate tracking and attribution algorithms, we expect to continue using the labeled sequence of contrails.

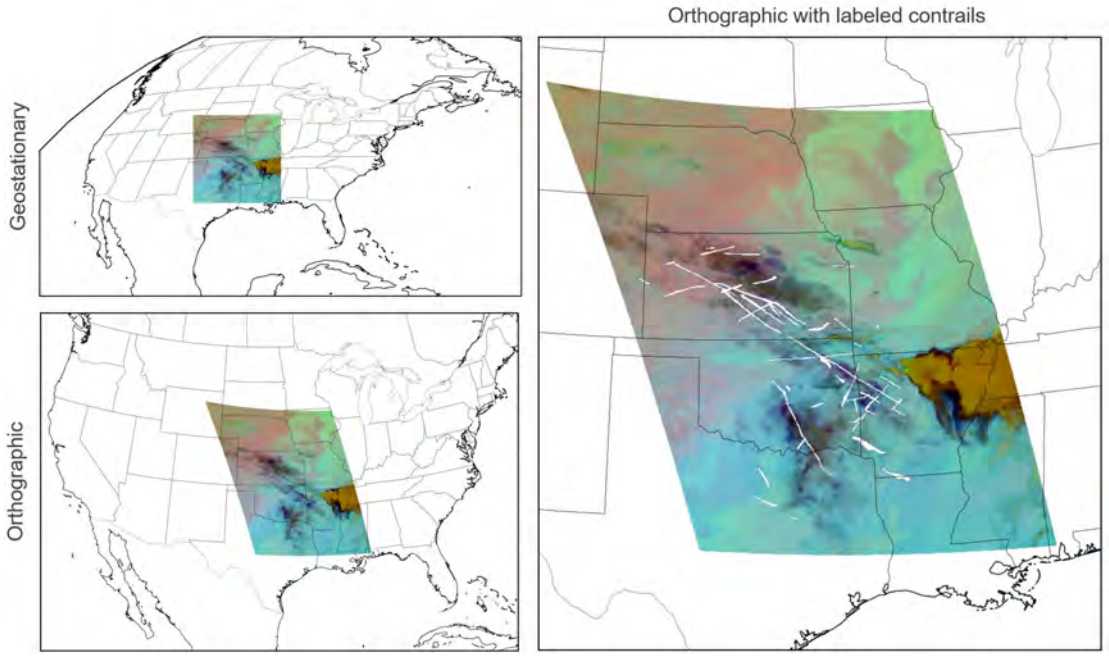

Figure 2.6. Ash transform of a Geostationary Operational Environmental Satellite 16 (GOES-16) mesoscale image on 2022-04-21 at 08:00 UTC. The geostationary image shows what is directly captured by GOES. We reproject the image to an orthographic projection centered on the contiguous United States to manually label the contrails (shown in white on the right plot). The time series is labeled from 08:00 to 10:00 UTC on 2022-04-21. This time series identifies over 100 contrails, which can each be tracked individually on the dataset.

Milestone

Milestone 2: Demonstrate first implementation of a contrail identification module to the FAA [*completed*].

Major Accomplishments

- Developed a KDE approach to extend contrail detections into an estimate of regional contrail formation likelihood
- Developed an approach to combine advected flight track data and contrail observations in order to evaluate the accuracy of contrail-forming region forecasts
- Created a validation dataset for contrail heights by collocating contrails detected by the GOES Advanced Baseline Imager and CALIOP instruments
- Evaluated the accuracy of the current state-of-the-art approach to contrail height estimation
- Began development of an improved height estimation approach including an uncertainty metric
- Developed a preliminary dataset of manually labeled contrails on a *sequence* of GOES images
- Began ground-truth evaluation of our Kalman filtering algorithm to enable more accurate filter tuning

Publications

None.

Outreach Efforts

An oral presentation was given by Vincent Meijer at the 5th International Conference on Transport, Atmosphere and Climate conference in Munich, Germany, hosted by the German Aerospace Center.

Authors: Vincent R. Meijer, Sebastian D. Eastham, Steven R. H. Barrett
Title: Using satellite-based observations of contrails to inform contrail avoidance strategies

One-sentence summary: Comparison of satellite-based observations of contrails with numerical weather prediction data indicates that forecasts of persistent contrails are lacking. Short-term approaches that utilize observational data of contrails are shown to outperform numerical weather prediction models.
Date: June 29, 2022
Publication status: N/A

Awards
None.

Student Involvement
The research for this task was primarily conducted by Vincent Meijer and Louis Robion, graduate research assistants at MIT. The communication of this research to the FAA was primarily conducted by Jad Elmourad, a graduate research assistant at MIT.

Plans for Next Period
- Extend KDE and flight density construction from 2D to 3D.
- Investigate the usage of larger-scale NWP variables to improve the contrail height estimation.
- Complete the development of a filtering method to ensure more accurate contrail detections, including operationalization.
- Finalize and deploy a contrail height estimation technique including an evaluation of accuracy and uncertainty.

References
Kox, S., Bugliaro, L., & Ostler, A. (2014). Retrieval of cirrus cloud optical thickness and top altitude from geostationary remote sensing. *Atmospheric Measurement Techniques*, *7*(10), 3233–3246. https://doi.org/10.5194/amt-7-3233-2014

Strandgren, J., Bugliaro, L., Sehnke, F., & Schröder, L. (2017). Cirrus cloud retrieval with MSG/SEVIRI using artificial neural networks. *Atmospheric Measurement Techniques*, *10*(9), 3547–3573. https://doi.org/10.5194/amt-10-3547-2017

Task 3 - Contrail Radiation Module
Massachusetts Institute of Technology

Objective
The objective of Task 3 is to develop a contrail radiation module. This module will evaluate the warming of individual contrails (both existing and counter-factual) by incorporating information on surface albedo, cloud cover, and other factors. The contrail radiation module enables us to assess the contrail impact of flight trajectories. Eventually, when integrated with the other modules, this module will allow us to extract climate-optimal contrail avoidance strategies.

Research Approach
In this task, we will develop two main capabilities: (a) simulating contrail formation, persistence, and evolution and (b), evaluating the radiative forcing impact of contrails. This module will initially be built on MIT's Aircraft Plume Chemistry, Emissions, and Microphysics Model (APCEMM) (Fritz et al., 2020) and the Contrail Evolution and Radiation Model (Caiazzo et al., 2017) and will incorporate recent advances in contrail radiative modeling (Sanz-Morère et al., 2020; Sanz-Morère et al., 2021). The radiative forcing impact evaluation will be built using Atmospheric Radiation Measurement's Rapid Radiative Transfer Model (RRTM) (Mlawer et al., 1995). Later versions will be calibrated and iteratively improved using measured contrail radiative effects from satellite observations, enabling improved cost–benefit assessments.

Overview
The flow chart in Figure 3.1 gives an overview of the various steps involved in the contrail radiation module, starting from a given trajectory and ending with the contrail climate impact of that trajectory.

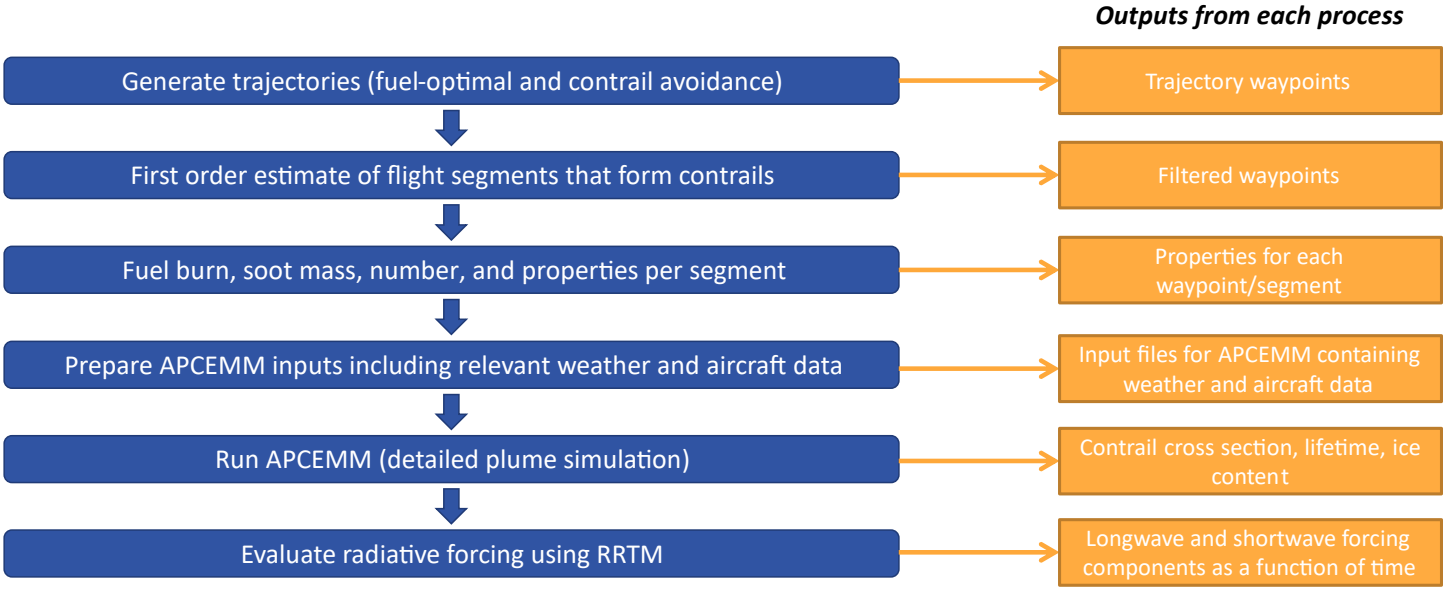

Figure 3.1. Overview of contrail radiation module: steps and outputs. APCEMM: Aircraft Plume Chemistry, Emissions, and Microphysics Model; RRTM: Rapid Radiative Transfer Model.

The contrail radiation module starts with an aircraft trajectory, which can be obtained from the trajectory planning module (see Task 4). This trajectory goes through a first-pass filter that estimates which segments of the flight will form persistent contrails according to the Schmidt–Appleman criterion and ice supersaturation criterion. For those segments, the fuel burn, soot mass, soot number, and other properties are obtained. Subsequently, the input files for APCEMM are prepared, which includes fetching the relevant weather and aircraft data. Then, the contrail plume is simulated by running APCEMM. The simulation outputs a time series of various plume properties, such as ice aerosol volume, particle number, surface area, horizontally and vertically integrated optical depths, etc. These outputs are then used to evaluate the time series' radiative forcing of the contrail using the RRTM.

Develop capabilities to simulate contrail formation, persistence, and evolution
The approach here was to embed APCEMM into a flexible "on-demand" tool to simulate contrails resulting from observed or anticipated flights.

The major modifications made to APCEMM during the implementation were related to the weather data. Because weather data are used across different modules (and tasks), the choice of weather data must be consistent across the modules. ERA5 from the European Centre for Medium-Range Weather Forecasts (ECMWF) was used in all of the other modules (contrail forecasting, contrail identification, and trajectory planning). However, the Modern Era Retrospective for Research and Analysis 2 (MERRA-2) product from NASA's Global Modeling and Assimilation Office was used in the initial implementation of the contrail radiation module. We then switched to ERA5, directly using the same meteorological variables from ECMWF when readily available and inferring those which were not readily available.

Table 3.1. Variables retrieved for use in the Aircraft Plume Chemistry, Emissions, and Microphysics Model (APCEMM) and Rapid Radiative Transfer Model (RRTM).

Variable	Unit	Used in
Eastward wind	m/s	APCEMM
Northward wind	m/s	APCEMM
Pressure	Pa	APCEMM / RRTM
Specific humidity	kg/kg	APCEMM / RRTM
Air temperature	K	APCEMM / RRTM
Geopotential	m^2/s^2	APCEMM / RRTM
Tropopause pressure	Pa	RRTM
Surface albedo for near infrared, diffuse	-	RRTM
Surface albedo for near infrared, direct	-	RRTM
Surface albedo for visible, diffuse	-	RRTM
Surface albedo for visible, direct	-	RRTM
Surface emissivity	-	RRTM
Fraction of cloud cover	-	RRTM
Specific cloud ice water content	kg/kg	RRTM
Specific cloud liquid water content	kg/kg	RRTM
Specific rain water content	kg/kg	RRTM
Specific ice water content	kg/kg	RRTM

Develop capabilities to evaluate the radiative forcing impact of contrails

We implemented a high-speed radiative impact estimation approach based on the results from APCEMM simulations, using the RRTM. We used 16 wavelength bands for the surface emissivity values that are part of the longwave forcing calculation.

Case study: Applying the contrail radiation module

We applied the full contrail radiation module to a set of simulated trajectories in order to verify that the components of the pipeline are well integrated. An example flight with its resulting contrail climate impact is shown in Figure 3.2, and an example of the more detailed outputs of the contrail radiation module are shown in Figure 3.3.

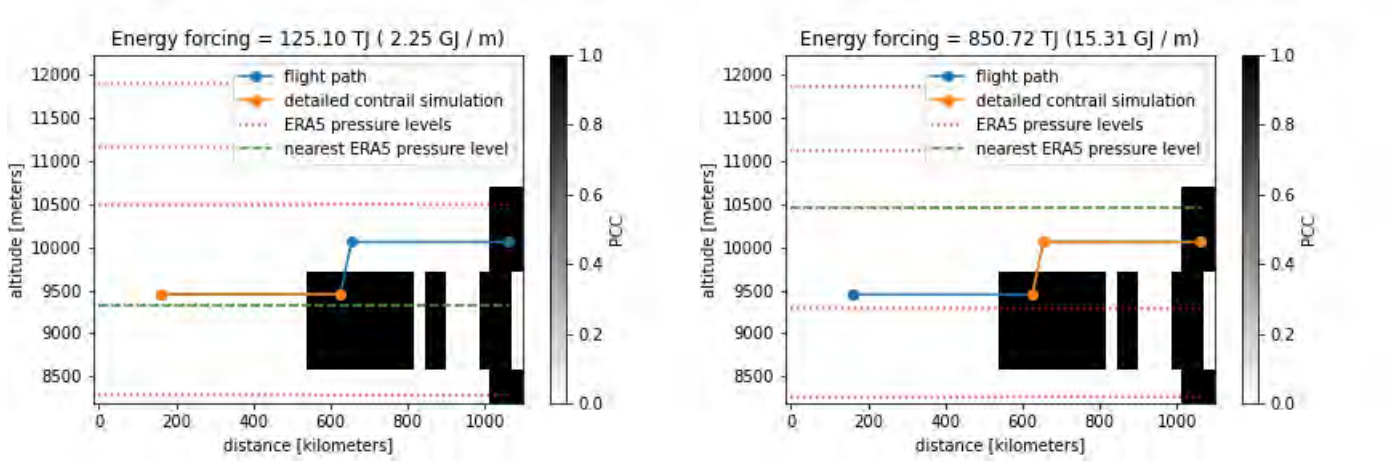

Figure 3.2. Example of applying the contrail radiation module to a flight trajectory. The trajectory is split into two parts (left and right). In each plot, the solid black region represents persistent contrail formation areas (PCFAs) (here, only a binary persistent contrail condition [PCC] map is considered), the blue line represents the flight trajectory, the orange line represents the section of the flight trajectory that is being considered, the dashed red lines represent the ECMWF Renalysis v5 (ERA5) pressure levels at which weather data are provided, and the green dashed line highlights the ERA5 pressure level that is nearest to the flight section under consideration. In the title of each subplot, the contrail energy forcing per contrail length is given as well as the total contrail energy forcing per flight segment.

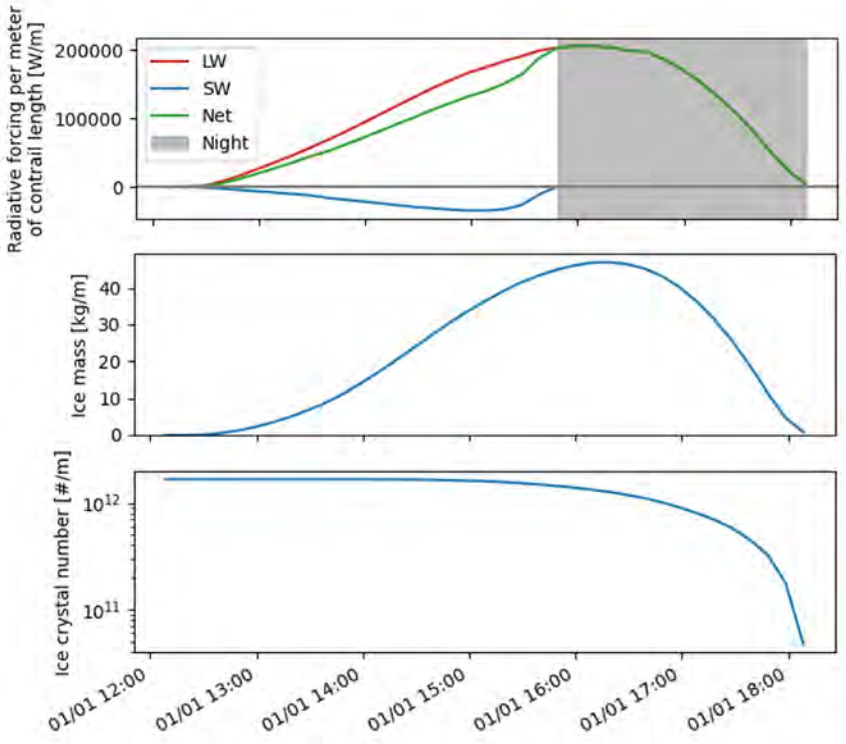

Figure 3.3. Example output from applying the contrail radiation module to one point along a flight trajectory. The top plot shows the radiative forcing impact of the contrail, separated into its warming longwave (LW) and cooling shortwave (SW) components. The x-axis is time. The middle plot shows the evolution of the contrail ice mass, and the bottom plot shows that of the contrail ice crystal number. All values are given per unit contrail distance.

Milestone

Milestone 3: Demonstrate a first implementation of the contrail radiation module to the FAA [*completed*].

Major Accomplishments

- Developed a pipeline to simulate contrail formation and evolution along projected flight tracks using an intermediate-fidelity contrail model (APCEMM)
- Integrated a radiative transfer model to run on the results from the APCEMM simulation
- Modified APCEMM and radiative impact estimation approach to use different meteorological data (ECMWF forecast instead of MERRA-2 reanalysis)
- Applied the entire contrail radiation pipeline (contrail plume simulation and radiative impact estimation) on a set of simulated trajectories output by the trajectory module
- Performed preliminary comparisons of the outputs of the contrail radiation module with other literature studies and models

These accomplishments will enable further development of the contrail radiation module in order to obtain a faster working module based on the heuristic approach described below.

Publications

None.

Outreach Efforts
None.

Awards
None.

Student Involvement
This task was primarily conducted by Jad Elmourad, a graduate research assistant at MIT.

Plans for Next Period
Heuristic approach

Applying the contrail radiation module to a set of trajectories made it clear that there is a large computational cost for running the plume simulation using APCEMM and the radiative forcing calculation using RRTM. In order to align with this project's goal of enabling near-real-time decision-making, we decided to pursue the development of a faster simulation approach that would not largely compromise accuracy. This approach will be based on *heuristics* derived from more detailed calculations, i.e., using the capabilities developed above.

References
Fritz, T. M., Eastham, S. D., Speth, R. L., & Barrett, S. R. H. (2020). The role of plume-scale processes in long-term impacts of aircraft emissions. *Atmospheric Chemistry and Physics*, *20*(9), 5697–5727. https://doi.org/10.5194/acp-20-5697-2020

Caiazzo, F., Agarwal, A., Speth, R. L., & Barrett, S. R. H. (2017). Impact of biofuels on contrail warming. *Environmental Research Letters*, *12*(11), 114013. https://doi.org/10.1088/1748-9326/aa893b

Sanz-Morère, I., Eastham, S. D., Allroggen, F., Speth, R. L., & Barrett, S. R. H. (2020). *Effect of contrail overlap on radiative impact attributable to aviation contrails* [Preprint]. Radiation/Atmospheric Modelling/Troposphere/Physics (physical properties and processes). https://doi.org/10.5194/acp-2020-181

Sanz-Morère, I., Eastham, S. D., Allroggen, F., Speth, R. L., & Barrett, S. R. H. (2021). Impacts of multi-layer overlap on contrail radiative forcing. *Atmospheric Chemistry and Physics*, *21*(3), 1649–1681. https://doi.org/10.5194/acp-21-1649-2021

Mlawer, E.J., Taubman, S.J., Clough, S.A. (1995). *RRTM: a rapid radiative transfer model* (Report No. PL-TR-96-2080, 278). Proceedings of the 18th Annual Conference on Atmospheric Tramission Models.

Task 4 - Trajectory Planning Module
Massachusetts Institute of Technology

Objective
The objective of Task 4 is to develop a trajectory planning module that will forecast fuel burn and emissions as a function of the spectrum of potential flight paths that will be taken. The initial version will consider conventional fuel, CO_2 emissions, and vertical altitude deviations, but each of these categories can be expanded in the future. The module will initially focus on one common aircraft type.

Research Approach
Development of trajectory optimization

As input, the trajectory optimization module will take an origin–destination pair, departure time, weather data, and airplane performance data. The module will then output a set of trajectories based on varying degrees of contrail avoidance. For each route, it will output the fuel burn, distance traveled through contrail-forming regions, and flight time.

ERA5 weather data from ECMWF will be used in the initial development; these data will primarily include temperature, relative humidity, and wind velocity. The former two meteorological variables have been used to determine the regions that form

persistent contrails; however, in the future, this submodule could be replaced with the contrail forecasting module (see Task 1).

MIT's Transport Aircraft System OPTimization (TASOPT) tool (Drela, 2011) was used to determine airplane and engine performance metrics such as fuel flow rates during climb and cruise, climb and descend rates, air–fuel ratios, true airspeed, and exhaust gas temperatures. A single aircraft type was used, with its performance metrics calculated for different operating conditions. The operating conditions were specified by the altitude and aircraft gross weight.

The optimization followed a graph-based approach in which a uniform-cost search algorithm was implemented. The airspace at cruise between the origin–destination airports was mapped onto a 2D grid. One dimension was the altitude, and the other dimension was the distance traveled along the lateral track. In this initial development phase, the lateral track of the aircraft was fixed to the great circle route; however, future implementations could expand this approach to allow for horizontal deviations.

The initial formulation of the cost function was a weighted sum of fuel burn and contrail length, as shown below.

$$J = C \times \theta + \mathrm{F} \times (1 - \theta)$$

where J is the cost function, C is the contrail length, F is the fuel burn, and θ is the tradeoff parameter that determines the degree of contrail avoidance.

$\theta = 0$: gives the baseline case, in which the flight is optimized for fuel burn
$\theta = 1$: gives the maximum contrail avoidance case

The parameter θ can be varied between 0 and 1 in order to simulate different degrees of contrail avoidance.

Application
We applied the trajectory planning module to a large set of global flights in order to assess the fuel burn penalty associated with contrail avoidance (targeted at contrail length minimization). We sampled 100,000 random flights from the 2019 flight schedule operated by a narrow-body aircraft fleet. The aircraft performance model was based on a single-aisle aircraft approximating the Boeing 737 MAX 9.

The results are shown in Figure 4.1. We found that 98% of contrail length can be avoided by exclusively using vertical re-routing. Furthermore, contrail avoidance costs an additional 0.3% in fuel on average, when considered from a fleet-wide perspective, and 1% in fuel if only the contrail-forming flights are considered.

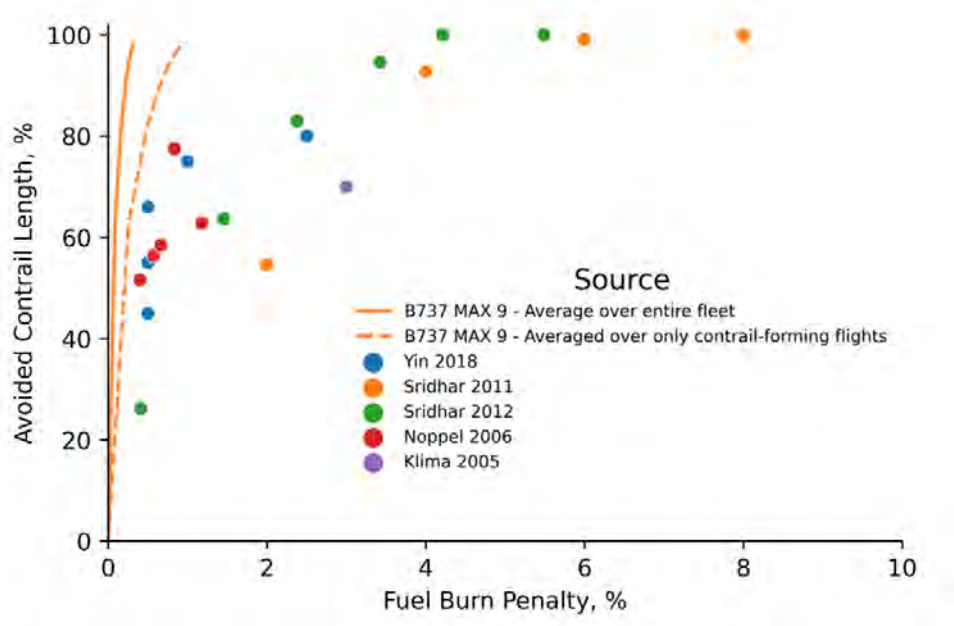

Figure 4.1. Tradeoff between avoided contrail length and fuel burn penalty for a Boeing 737 MAX 9 for a full year of global operations. The results are presented for two cases: for the entire fleet (solid line) and for only contrail-forming flights (dashed line). Results from other studies are included for comparison, even though the studies differ in their approach (type of deviation, fuel model, weather data, region, routes, and scale).

Furthermore, we studied the impact of constraining the maximum fuel penalty per flight. We found that limiting the maximum fuel penalty per flight to 5% did not significantly affect the amount of contrail reduction obtained. Imposing this limit reduced the avoided contrail length by 0.9% and the fleet-wide fuel burn penalty by <0.1%. However, this step ensures that no single flight is encouraged to make large deviations, reducing the possibility of a large inadvertent penalty. This is particularly important given the level of uncertainty in PCFA predictions.

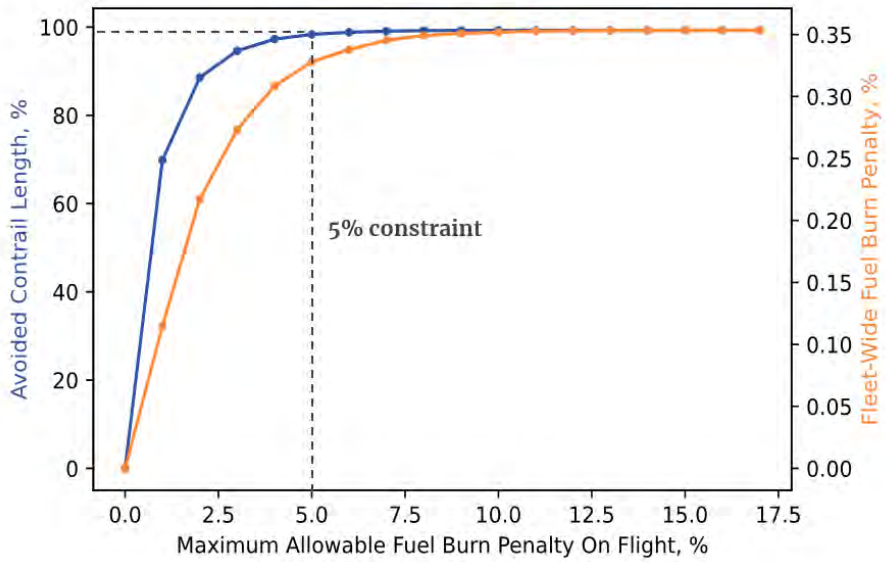

Figure 4.2. Impact of constraining the maximum fuel penalty per flight. The x-axis shows the fuel penalty constraint that was applied. The left axis and blue line show the percentage of contrail length avoided. The right axis and orange line show the fleet-wide fuel burn penalty.

At this stage, the trajectory planning module is focused on contrail length minimization. However, we intend to integrate this module with the contrail radiation module to develop the capability for trajectory optimization focused on climate impact (contrail and CO_2 energy forcing). For this purpose, we will combine both the current trajectory planning and contrail radiation modules in an optimization loop with multiple hierarchical levels. The trajectory planning component will generate trajectories and determine the order for exploring possible trajectories according to the best-known contrail impacts at the time. These trajectories will then be passed to the contrail radiation component, which will refine the estimates of the contrail impacts and send them back to the trajectory planning component. This procedure will loop until certain convergence criteria are reached.

Milestone

Milestone 4: Demonstrate the first implementation of a trajectory optimization module to the FAA [*completed*].

Major Accomplishments

- Developed a trajectory model to simulate flights with differing degrees of contrail avoidance
- Performed preliminary estimates of the fuel burn penalty associated with limited vertical deviations using weather data

Publications

None.

Outreach Efforts

A poster presentation on ASCENT 78 was delivered to the 5th International Conference on Transport, Atmosphere and Climate conference in Munich, Germany, hosted by the German Aerospace Center.

Authors: Jad Elmourad, Sebastian D. Eastham, Raymond L. Speth, Florian Allroggen, Steven R. H. Barrett
Title: Flight Level Optimization for Contrail Avoidance
One-sentence summary: Preliminary results regarding the contrail–CO_2 tradeoffs associated with contrail avoidance.
Date: June 27–30, 2022
Publication status: N/A (poster presentation)

FAA support was acknowledged.

Awards

None.

Student Involvement

This task was primarily conducted by Jad Elmourad, a graduate research assistant at MIT.

Plans for Next Period

- Integrate the contrail forecasting module after it is completed to replace the current calculation of PCCs.
- Extend the module to incorporate lateral deviations.
- Integrate this module with the contrail radiation module in order to directly optimize for climate impact.

References

Drela, M. (2011). *Development of the D8 Transport Configuration*. 29th AIAA Applied Aerodynamics Conference. Honolulu, HI.

Greitzer, E. M., Bonnefoy, P., De la Rosa Blanco, E., Dorbian, C., Drela, M., Hall, D., Hansman, R., Hileman, J., Liebeck, R., Lovegren, J., Mody, P., Pertuze, J., Sato, S., & Spokovsky, Z., Tan, C. (2010). *N + 3 Aircraft Concept Designs and Trade Studies, Final Report Volume 1* (Report No. 2010-216794/VOL1). NASA Technical Reports 2, 216794.